Available online at www.sciencedirect.com

ScienceDirect

Energy Procedia 158 (2019) 4861–4869

Energy Procedia

www.elsevier.com/locate/procedia

10th International Conference on Applied Energy (ICAE2018), 22-25 August 2018, Hong Kong, China

Magnesium oxide from natural magnesite samples as thermochemical energy storage material

Christian Knoll[a,b], Danny Müller[a,*], Werner Artner[c], Jan M. Welch[d], Elisabeth Eitenberger[e], Gernot Friedbacher[e], Andreas Werner[f], Peter Weinberger,[a] Michael Harasek[b]

[a] *Institute of Applied Synthetic Chemistry, TU Wien, Getreidemarkt 9, 1060 Vienna, Austria.*
[b] *Institute of Chemical, Environmental & Biological Engineering, TU Wien, Getreidemarkt 9, 1060 Vienna, Austria.*
[c] *X-Ray Center, TU Wien, Getreidemarkt 9, 1060 Vienna, Austria*
[d] *Atominstitut, TU Wien, Stadionallee 2, 1020 Vienna, Austria.*
[e] *Institute of Chemical Technologies and Analytics, TU Wien, Getreidemarkt 9/164, 1060 Vienna, Austria*
[f] *Institute for Energy Systems and Thermodynamics, TU Wien, Getreidemarkt 9, 1060 Vienna, Austria.*

Abstract

Thermochemical energy storage based on the $Mg(OH)_2$ / MgO cycle is considered as attractive process for recycling of industrial waste heat between 350-400 °C. Based on a recent study, revealing $MgCO_3$-derived MgO as highly attractive starting material for such a storage cycle, three different natural magnesites were investigated to analyze the process-performance using industrially available raw-materials. Whereas, the varying amounts of Ca^{2+} and Fe^{2+} as major impurities did not notably affect the reactivity / cycle stability within the series, compared to the analytically pure reference material a notable decrease of performance was evidenced.

Keywords: magnesite; magnesium oxide; hydration reactivity; *in-situ* X-Ray powder diffraction; thermochemical energy storage

1. Introduction

A variety of inorganic materials is reversibly decomposed above their equilibrium temperature forming a solid residue and a gaseous by-product. As the reaction is reversible, an exothermic back reaction occurs below the decomposition temperature in the presence of the formerly released gas. Due to the inherent consumption of energy / heat on decomposition, and its release during recombination, such reversible chemical reactions attracted scientific interest for their application in thermal energy storage. [1, 2]

Although, latent [3] or sensible [4] heat storage is already a commercialized technology for thermal energy storage,

10.1016/j.egypro.2019.01.707

a thermochemical energy storage (TCES) approach using reversible chemical reactions could be attractive for complementary purposes, where latent or sensible heat storage are less efficient or even unsuitable. [5] The major advantage of TCES-materials compared to the so far established thermal energy storage systems is on the one hand a notably higher storage density and a loss-less storage (in the absence of the reactive gas no backreaction, thus discharging occurs), but even more the large operable temperature window. [6]

Depending on the selected material, categorized according to the involved reactive gas as *e.g.* H_2O, NH_3, H_2 CO_2, O_2, waste heat levels between approximately 50 – 1200 °C may be addressed. The lower limits are realized by salt hydrates, suitable for energy-efficient smart housing concepts, [7, 8] whereas on the other end carbonates and oxides allow for *e.g.* combination with concentrating solar power plants (CSP) to bridge non-operational times. [9, 10] In the medium-temperature level between 250-500 °C a variety of industrial waste heat sources is compatible with *e.g.* hydroxide / oxide equilibria. [11, 12] One major criterion for application of a TCES-process on an industrial scale is the availability of the involved raw-material in massive quantities to an attractive price. In this context, especially $Mg(OH)_2$ / MgO used on industrial scales as raw-material for refractories or cement [13] would be an attractive candidate. The operational temperature of the $Mg(OH)_2$ / MgO couple with 350-400 °C would also perfectly fit the industrial demands. [12, 14]

Considering these boundary conditions, several studies focused on various aspects of the rehydration reaction of MgO, as *e.g.* fundamental reactivity [15] and kinetics, [16, 17] a suitable reactor setup, [18] application as a heat pump, [19-22] and las but not least an enhancement of the materials' reactivity. Especially the aim for a higher reactivity of the material is crucial for its application in TCES, as compared to the homologous $Ca(OH)_2$ / CaO system [11] the performance in regard of reaction rate and completeness is worse.[a] Composite materials for a better thermal conductivity, [23, 24] the addition of lithium salts [25-27] or even a dotation of MgO with Ca^{2+} [28] were reported to enhance the performance. Scientifically valid and highly interesting, nevertheless all these modifications must be considered as pure academic approach, as the correlated costs outweigh the advantage of $Mg(OH)_2$ / MgO as cost-efficient TCES-material and thereby impede an application of those modified materials on an industrial scale.

The reactivity of the MgO is notably affected by the chemical history / particle morphology of the precursor material, thus a $Mg(OH)_2$- based MgO reacts differently than a MgO derived from $MgC_2O_4{\cdot}2H_2O$ or $MgCO_3$. Especially $MgCO_3$-based MgO has a higher reactivity and much better cycle stability than the $Mg(OH)_2$-based MgO. As magnesite ($MgCO_3$) is also industrially used as raw-material for the preparation of MgO, this could direct to an industrial feasibility of the process.

To prevent any interfering effects of impurities or naturally present secondary phases, and thus simplify the characterization, so far most studies used analytically pure materials. On an industrial scale only naturally occurring material, in this case naturally abundant magnesite, could be used as raw-material in a TCES-process. Therefore, herein three different naturally occurring magnesite samples, used in industrial processes for cement or refractory production, were investigated regarding their performance in a thermochemical energy storage process and compared to the previously obtained results for analytically pure $MgCO_3$.

2. Experimental Methodology

2.1 Material

Three natural magnesite samples **A1**, **B1** and **C1**, having a particle size below 65µm were used. Most common foreign ions are Ca^{2+} and Fe^{2+}, so the three samples were selected to cover both a variable range of Ca^{2+}- and Fe^{2+} content:

- Magnesite **A1**: 2.05 % CaO, 0.31 % Fe_2O_3
- Magnesite **B1**: 1.95 % CaO, 6.57 % Fe_2O_3
- Magnesite **C1**: 11.06 % CaO, 5.95 % Fe_2O_3

[a] The application of $Ca(OH)_2$ / CaO instead of $Mg(OH)_2$ / MgO is hampered for may purposes due to the notably higher decomposition temperature of $Ca(OH)_2$ around 600 °C.

2.2 X-Ray Powder Diffraction

The powder X-ray diffraction measurements were carried out on a PANalytical X'Pert Pro diffractometer in Bragg-Brentano geometry using Cu $K_{\alpha 1,2}$ radiation and an X'Celerator linear detector with a Ni-filter. For *in-situ* monitoring of experiments an Anton Paar XRK 900 reaction chamber was used. The sample was mounted on a hollow ceramic powder sample holder, allowing for complete perfusion of the sample with the reactive gas. The sample temperature is controlled directly via a NiCr-NiAl thermocouple and direct environmental heating. The reactive gas flow was set to 0.2 L min^{-1}, unless otherwise stated. For the *in-situ* observation of the rehydration reactivity 3 ml min^{-1} water (provided by a HPLC-pump) was passed through an evaporation coil kept at 300 °C. The resulting 3 g min^{-1} steam were mixed with 0.2 L min^{-1} helium as carrier gas (H_2O partial pressure equals 0.96 bar) and passed from the top through the sample. The carrier gas is necessary to force the steam transfer through the system. During rehydration the sample warmed to around 65 °C. Between the consecutive rehydration cycles the *in-situ* formed $Mg(OH)_2$ was calcined at 375 °C for 15 minutes directly in the reaction chamber of the P-XRD. As the sample is completely penetrated by the X-rays, the obtained diffractograms are an average through the complete sample. The diffractograms were evaluated using the PANalytical program suite HighScorePlus v3.0d. A background correction and a $K_{\alpha 2}$ strip were performed. Phase assignment is based on the ICDD-PDF4+ database, the exact phase composition was obtained via Rietveld-refinement in the program suite HighScorePlus v3.0d. All quantifications based on P-XRD are accurate within of ±5 %.

2.3 Scanning electron microscopy (SEM)

SEM images were recorded on gold coated samples with a Quanta 200 SEM instrument from FEI under low-vacuum at a water vapor pressure of 80 Pa to prevent electrostatic charging.

2.4 BET-specific surface area analyzer

The specific surface of the samples was determined by nitrogen sorption measurements, which were performed on an ASAP 2020 (Micromeritics) instrument. The samples (amounts between 100-200 mg) were degassed under vacuum at 80 °C overnight prior to measurement. The surface area was calculated according to Brunauer, Emmett and Teller (BET). [29]

3. Results and Discussion

Based on former experience with calcination of $MgCO_3$, the natural samples (scheme 1, **A1-C1**) were calcined at 600 °C under a static atmosphere of air for 4 h, resulting the corresponding samples of MgO (scheme 1, **A2-C2**). The increased Fe^{2+}-content in magnesite B and C is also evidenced from the slight orange shade of the samples **B2** and **C2** after calcination (see figure A1).

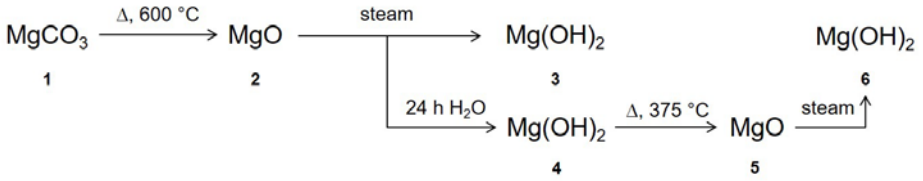

Scheme 1. Calcination / rehydration flow-chart applied for the characterization of the natural magnesite samples.

From previous work on $MgCO_3$-derived MgO it is known, that directly calcined MgO (MgO **2** in scheme 1) would exhibit no, or only a very limited reactivity towards steam during attempted rehydration to $Mg(OH)_2$. Therefore, MgO **2** was rehydrated in liquid water for 24 h and afterwards calcined for 4 h at 375 °C. [15]

The BET-surfaces of the magnesite-precursors (**A1-C1**) and of the different MgO samples **A2-C2** and **A5-C5** were

compared to anticipate the rehydration reactivity. [30]

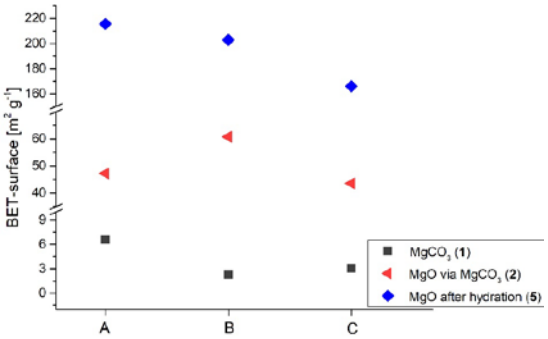

Figure 1. Specific surfaces of the different MgO-species derived from magnesite samples **A**, **B** and **C**. Numerical values are given in table A1.

The surface area for highly reactive MgO species obtained by calcination of $Mg(OH)_2$ varies between 250 – 300 $m^2\ g^{-1}$, [30] whereas, using analytically pure $MgCO_3$ for the resulting MgO values up to 160 $m^2\ g^{-1}$ were reported. Using the natural magnesites, for the directly calcined MgO notably lower values – indicating a poor reactivity – were obtained (red symbols in figure 1). In contrast, after hydration in liquid water and subsequent calcination (blue symbols) the found specific surfaces were found even higher than for identically treated MgO originating from analytically pure $MgCO_3$.

To correlate the specific surface of the various samples to the rehydration reactivity, MgO was reacted in the P-XRD, allowing for *in-situ* observation of the $Mg(OH)_2$ formation. In figure 2 the rehydration behavior for the MgO samples **A2-C2** is compared.

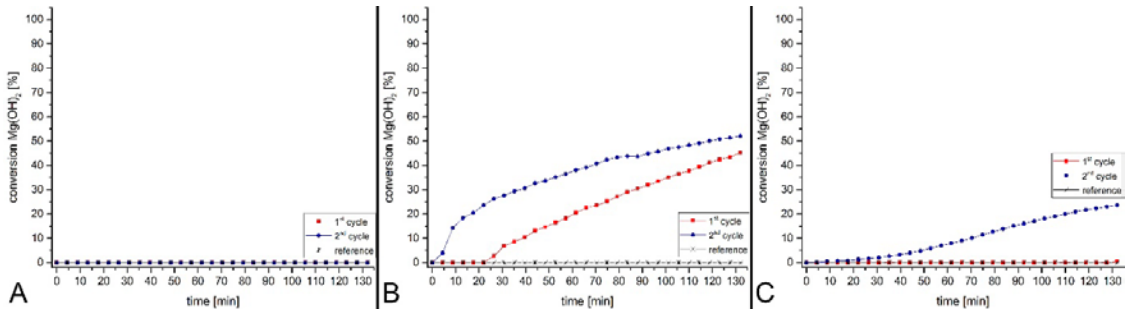

Figure 2. Conversion plots derived from the *in-situ* powder X-Ray diffraction during hydration of samples **A2** (left), **B2** (middle) and **C2** (right). The typical conversion for an equivalent sample, derived from analytically pure $MgCO_3$ is given as reference. (Rehydration conditions: 3 g min^{-1} steam, 0.2 L min^{-1} He)

The rehydration reactivity of samples **B2** and **C2** was quite unexpected, as from the BET-data and the previous experience with $MgCO_3$-derived MgO for all three samples no conversion to the hydroxide was expected at this stage. So far, all $MgCO_3$-derived MgO samples needed a prior rehydration step in liquid water, before the anew calcined material would be reactive towards steam, forming the hydroxide. In the actual case this assumption was only partially confirmed by displaying a higher reactivity towards steam in the second rehydration cycle. As most reactive material was identified **B2**, resulting a conversion of 52.1 % for the second cycle.

From a chemical point of view the presence of 6.57 % Fe^{2+} in sample **B2** does not really explain this unexpected reactivity. Therefore, for a possible explanation the morphology of the three materials was compared in the SEM.

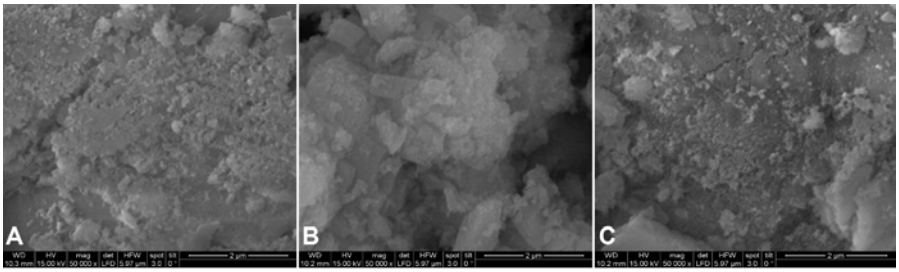

Figure 3. SEM-images of the MgO samples **A2** (left), **B2** (middle) and **C2** (right).

The SEM-images for the three freshly calcined magnesite samples revealed, that the original particle morphology of the magnesites **A1**, **B1** and **C1** (figure A2) had been mostly retained during calcination. Calcination had caused a further decrease of the particle size for sample **A1** whereas, for **B1** and **C1** (with an increased fraction of smaller particles) the structure was retained. Based on the SEM-images, the reason for the unexpected reactivity of **B1** most likely was attributed to the structured particle morphology, whereas for **A1** completely, and for **C1** to a major extent a fragmentation of the particles had occurred.

A notably different picture was obtained when analyzing the SEM-images of the samples after 24 h rehydration in water (**A3**-**C3**).

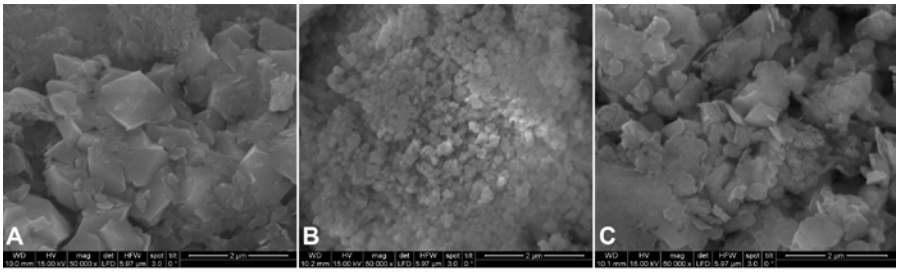

Figure 4. SEM-images of the magnesite samples **A3** (left), **B3** (middle) and **C3** (right).

The liquid water treatment over 24 h resulted in a notable reorganization of the particle morphology for all three samples, inverting the prior observation: Whereas especially in **A3**, but also in **C3** well-shaped crystallites had formed, **B3** had converted to tiny agglomerates of smallest particles. Particularly interesting and unprecedented may be considered the particle shape of the materials: $Mg(OH)_2$ adopts a very characteristic morphology, consisting of hexagonal brucite platelets aggregating along their basal plane. The morphology observed in figure 4 is notably different for all three samples, consisting of spherical particles with clearly shaped edges. Thermal treatment during calcination of the material at 375 °C for 4 h, leading to the MgO-samples **A4**-**C4**, even promoted the initiated process, as derived from the SEM-images shown in figure 5.

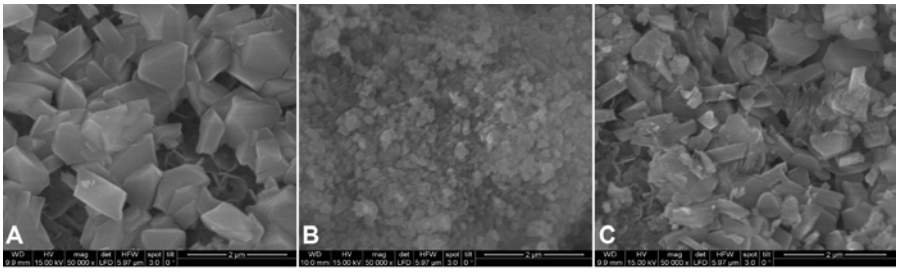

Figure 5. SEM-images of the magnesite samples **A5** (left), **B5** (middle) and **C5** (right).

Although, according to the SEM-images in figure 5 the MgO-samples **A5-C5** feature a notably different particle morphology, the BET-surfaces (figure 1, table A1) between 165 $m^2 g^{-1}$ (**C5**) and 215 $m^2 g^{-1}$ (**A5**) direct for all three samples towards a promising rehydration reactivity in the presence of steam. To investigate also the cycle stability of the materials, the MgO-samples **A5-C5** where subjected 5 consecutive rehydration / calcination cycles with *in-situ* determination of the phase-composition in the P-XRD setup. The intermediate calcination steps were realized directly in the reaction chamber of the P-XRD, heating the sample for 15 minutes to 375 °C in a stream of 0.2 L min^{-1} helium without introduction of moisture.

A comparison of rehydration reactivity and cycle stability of the three MgO samples **A5-C5** is shown in figure 6.

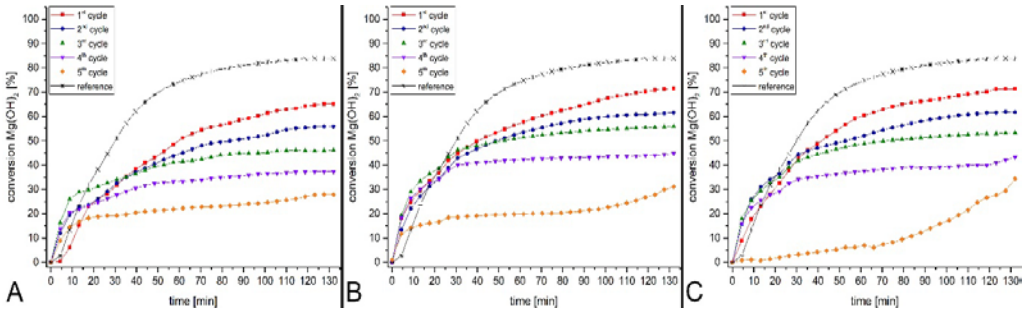

Figure 6. Conversion plots derived from the *in-situ* powder X-Ray diffraction during hydration of samples **A5** (left), **B5** (middle) and **C5** (right) for 5 consecutive cycles. The typical conversion for an equivalent sample, derived from analytically pure $MgCO_3$ is given as reference. (Rehydration conditions: 3 g min^{-1} steam, 0.2 L min^{-1} He)

Comparing the results shown in figure 6, a quite comparable and very similar rehydration reactivity and cycle stability is evidenced for the samples **A5-C5**. All of them feature a notable decrease of overall-conversion from the 1st to the 5th cycle, **C5** having an anomalous strong decrease of reactivity between the 4th and 5th cycle. For all three samples after rehydration (A6-C6) in the SEM a platelet type morphology – still lacking the characteristic hexagonal brucite shape – is observed (figure A3).

Compared to the reference, resulting 84 % formed $Mg(OH)_2$ within the first cycle, the maximum conversion for the natural magnesite derived MgO samples is lower, **B5** and **C5** yielding both 71.5 %, **A5** only 65.5 % $Mg(OH)_2$. The decrease during the 5 cycles to around 30 % is for the natural samples by far more pronounced than in the case of the reference material (62.7 %). In figure 7 each 1st and 5th cycle for the samples **A5-C5**, including the reference material is given for a better visualization.

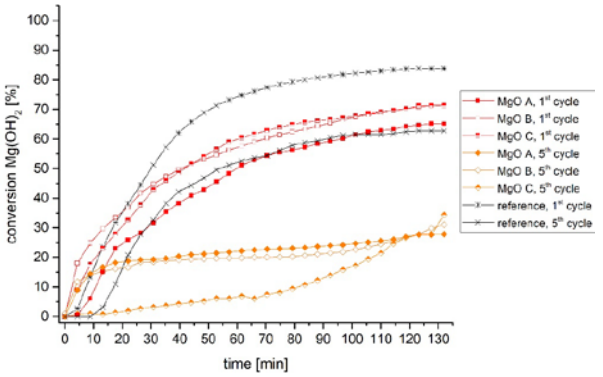

Figure 7. Conversion plots derived from the *in-situ* powder X-Ray diffraction for the 1st and 5th cycles of the three magnesite-derived MgO samples **A5-C5** and the corresponding reference material from analytically pure $MgCO_3$

The outcome of the conversion and especially cycle-stability tests of the natural magnesite-derived MgO material summarized in figure 7 reveals sobering regarding the performance of the materials suitable for a TCES-process based

on $Mg(OH)_2$ / MgO on a technological scale. Whereas, the initial reactivity of the materials was slightly worse than for an analytically pure $MgCO_3$-based MgO sample, the poor cycle stability over 5 consecutive rehydration / calcination cycles is a major issue. A process with a lower overall-conversion may be feasible under properly selected boundary conditions, but not in combination to a material degradation within 5 cycles to 50 % of the initial activity. $MgCO_3$ was selected as precursor for the MgO used in the $Mg(OH)_2$ / MgO TCES-cycle as previous studies revealed, that the thereby obtained MgO displayed a much higher reactivity than a $Mg(OH)_2$-derived material. In the case of the natural magnesites this effect could not be confirmed based on the present experimental data.

An interesting finding of this comparative study is the observation, that the reactivity / conversion of the various samples is only minorly affected by the increased amounts of unreactive $CaCO_3$ and Fe^{2+}-impurities within the series.[b] Nevertheless, as based on the specific surface of the samples' and their among each other comparable morphology no real explanation for the inferior performance in rehydration reactivity compared to a MgO-sample derived from analytically pure $MgCO_3$ is found, the source of the different performance may be located in the secondary phases of the magnesite-derived samples. As the series with $CaCO_3$-contents between 1.95 – 11.06 % and Fe^{2+}-contents between 0.31 – 6.57 % provides similar performance, even low amounts of foreign ions seem to deteriorate the reactivity of the material.

4. Conclusion

Natural magnesite samples were thermally decomposed to MgO, which was investigated for its performance in a $Mg(OH)_2$ / MgO thermochemical energy storage (TCES) cycle. The reaction conditions during calcination / rehydration of the samples were the same as for a recent study using analytically pure $MgCO_3$ as MgO-precursor, revealing a notable improvement rehydration reactivity of the material compared to a $Mg(OH)_2$-derived MgO.

Comparison of the rehydration reactivity, cycle stability and particle morphology of the magnesite-derived MgO resulted in following key-findings:

- The reactivity of the magnesite-derived MgO samples is comparable within the series (between 65-75 % $Mg(OH)_2$-formation), but lower than for the reference sample from analytically pure $MgCO_3$ with 84 % conversion.
- Also the cycle stability is comparable within the series, again inferior than for the reference sample (conversion depletes within the series to about 30 %, for the reference to 63 %).
- The natural magnesite-derived MgO-samples form during rehydration in liquid water after the initial calcination a $Mg(OH)_2$-phase with well-shaped crystallites, lacking the typical brucite-type hexagonal platelet morphology. The shape is retained during anew calcination.
- As from the specific surface, chemical behavior and particle morphology no sound explanation for the inferior reactivity towards an analytically pure reference material is found, the reason is found in the present impurities. It appears, as even impurities below 2 % Ca^{2+} and 0.3 % Fe^{2+} notably hamper the rehydration reactivity and cycle stability of magnesite-derived MgO.

The aim of the herein reported work was a feasibility study on the application of natural magnesites, used in industrial processes, for thermochemical energy storage purposes based on the $Mg(OH)_2$ / MgO cycle. Based on the obtained results it may be concluded, that only pure materials are feasible for a successful application in TCES, which derogates attractiveness and financial rentability of such a process on industrial scales.

5. Acknowledgement

This work was financially supported by the Austrian Research Promotion Agency (FFG Forschungsförderungsgesellschaft), project 845020, 841150 and project 848876. The X-Ray center (XRC) of the Vienna University of Technology provided access to the powder X-Ray diffractometer.

[b] The conversion curves displayed within this study are so far uncorrected for the amount of inactive material, so by its consideration the final yields of $Mg(OH)_2$ would be slightly higher.

6. Appendix

Table S1. Specific surfaces of the different MgO-species derived from magnesite samples **A**, **B** and **C**

	Magnesite **A**	Magnesite **B**	Magnesite **C**
$MgCO_3$ (**1**)	6.61	2.27	3.08
MgO via $MgCO_3$ (**2**)	47.23	60.76	43.55
MgO after hydration (**5**)	215.61	202.83	165.98

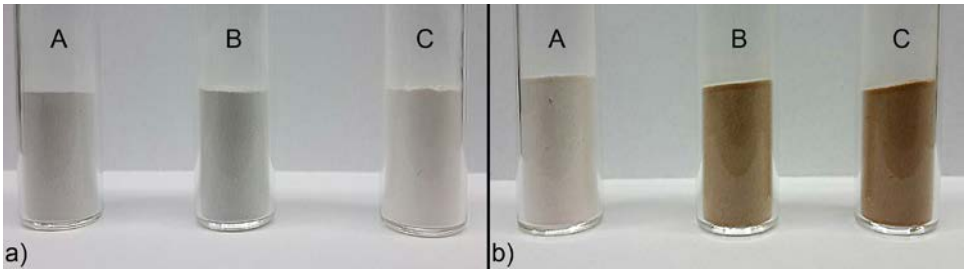

Figure A1. Natural magnesite samples **A-C** a) before calcination b) after calcination

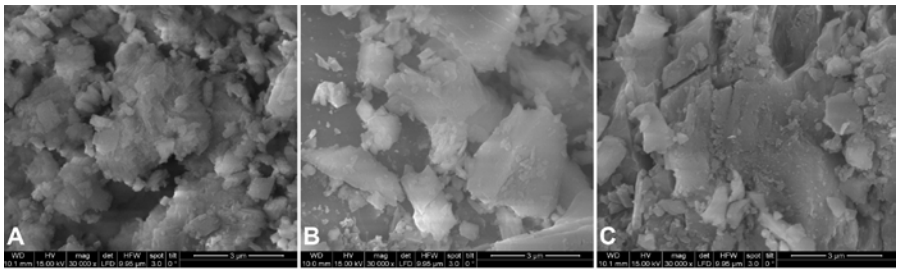

Figure A2. SEM-images of the magnesite samples **A1** (left), **B1** (middle) and **C1** (right).

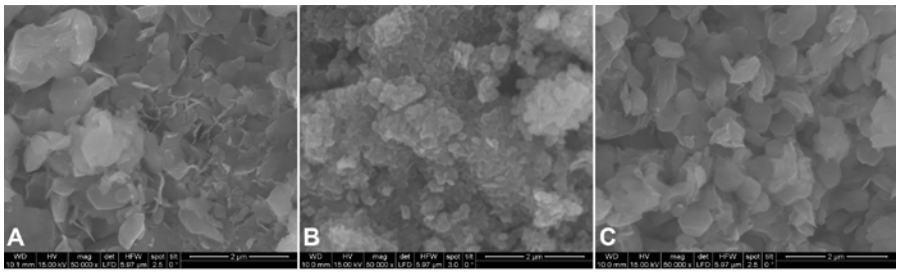

Figure A3. SEM-images of the samples **A6** (left), **B6** (middle) and **C6** (right) after 5 consecutive rehydration / calcination cycles in the P-XRD.

7. References

[1] T. Bauer, W.-D. Steinmann, D. Laing, R. Tamme, Thermal Energy Storage Materials and Systems, Annual Review of Heat Transfer, 15 (2012) 131-177.
[2] H. Zhang, J. Baeyens, G. Cáceres, J. Degrève, Y. Lv, Thermal energy storage: Recent developments and practical aspects, Progress in Energy and Combustion Science, 53 (2016) 1-40.
[3] B. Zalba, J.M. Marín, L.F. Cabeza, H. Mehling, Review on thermal energy storage with phase change: materials, heat transfer analysis and applications, Applied Thermal Engineering, 23 (2003) 251-283.
[4] R.Z.W. J. Xu, Y. Li, A review of available technologies for seasonal thermal energy storage, Solar Energy, (2014) 610-638.

[5] A. Dinker, M. Agarwal, G.D. Agarwal, Heat storage materials, geometry and applications: A review, Journal of the Energy Institute, (2015).
[6] A.H. Abedin, M.R. Rosen, A Critical Review of Thermochemical Energy Storage Systems, The Open Renewable Energy Journal, 4 (2011) 42-46.
[7] V.M. van Essen, J. Cot Gores, L.P.J. Bleijendaal, H.A. Zondag, R. Schuitema, M. Bakker, W.G.J. van Helden, Characterization of Salt Hydrates for Compact Seasonal Thermochemical Storage, (2009) 825-830.
[8] C. Knoll, D. Müller, W. Artner, J.M. Welch, A. Werner, M. Harasek, P. Weinberger, Probing cycle stability and reversibility in thermochemical energy storage – CaC2O4·H2O as perfect match?, Applied Energy, 187 (2017) 1-9.
[9] G. Ervin, Solar heat storage using chemical reactions, Journal of Solid State Chemistry, 22 (1977) 51-61.
[10] S. Kuravi, Y. Goswami, E.K. Stefanakos, M. Ram, C. Jotshi, S. Pendyala, J. Trahan, P. Sridharan, M. Rahman, B. Krakow, Thermal Energy Storage for Concentrating Solar Power Plants, Technology & Innovation, 14 (2012) 81-91.
[11] M. Linder, C. Roßkopf, M. Schmidt, A. Wörner, Thermochemical Energy Storage in kW-scale based on CaO/Ca(OH)2, Energy Procedia, 49 (2014) 888-897.
[12] Y. Kato, R. Takahashi, T. Sekiguchi, J. Ryu, Study on medium-temperature chemical heat storage using mixed hydroxides, International Journal of Refrigeration, 32 (2009) 661-666.
[13] M.A. Shand, The Chemistry and Technology of Magnesia, John Wiley & Sons Inc., Hoboken, New Jersey, (2006).
[14] Z. Pan, C.Y. Zhao, Dehydration/hydration of MgO/H2O chemical thermal storage system, Energy, 82 (2015) 611-618.
[15] D. Müller, C. Knoll, W. Artner, J.M. Welch, N. Freiberger, R. Nilica, M. Schreiner, M. Harasek, K. Hradil, A. Werner, P. Weinberger, An in-situ powder X-Ray diffraction study on the rehydration-reactivity of low temperature calcined Mg(OH)2, Applied Energy, submitted (2017).
[16] V.S. Birchal, S.D.F. Rocha, M.B. Mansur, V.S.T. Ciminelli, A simplified mechanistic analysis of the hydration of magnesia, The Canadian Journal of Chemical Engineering, 79 (2001) 507-511.
[17] H. Kuleci, C. Schmidt, E. Rybacki, E. Petrishcheva, R. Abart, Hydration of periclase at 350 ∘ C to 620 ∘ C and 200 MPa: experimental calibration of reaction rate, Mineralogy and Petrology, 110 (2016) 1-10.
[18] Y. Kato, F. Takahashi, A. Watanabe, Y. Yoshizawa, Thermal Performance of a Packed Bed Reactor of a Chemical Heat Pump for Cogeneration, Chemical Engineering Research and Design, 78 (2000) 745-748.
[19] Y. Kato, K. Kobayashi, Y. Yoshizawa, Durability to repetitive reaction of magnesium oxide/water reaction system for a heat pump, Applied Thermal Engineering, 18 (1998) 85-92.
[20] Y. Kato, Y. Sasaki, Y. Yoshizawa, Magnesium oxide/water chemical heat pump to enhance energy utilization of a cogeneration system, Energy, 30 (2005) 2144-2155.
[21] E. Mastronardo, L. Bonaccorsi, Y. Kato, E. Piperopoulos, C. Milone, Efficiency improvement of heat storage materials for MgO/H2O/Mg(OH)2 chemical heat pumps, Applied Energy, 162 (2016) 31-39.
[22] M. Zamengo, J. Ryu, Y. Kato, Thermochemical performance of magnesium hydroxide–expanded graphite pellets for chemical heat pump, Applied Thermal Engineering, 64 (2014) 339-347.
[23] A. Shkatulov, J. Ryu, Y. Kato, Y. Aristov, Composite material "Mg(OH)2/vermiculite": A promising new candidate for storage of middle temperature heat, Energy, 44 (2012) 1028-1034.
[24] M. Zamengo, J. Ryu, Y. Kato, Composite block of magnesium hydroxide – Expanded graphite for chemical heat storage and heat pump, Applied Thermal Engineering, 69 (2014) 29-38.
[25] H. Ishitobi, N. Hirao, J. Ryu, Y. Kato, Evaluation of Heat Output Densities of Lithium Chloride-Modified Magnesium Hydroxide for Thermochemical Energy Storage, Industrial & Engineering Chemistry Research, 52 (2013) 5321-5325.
[26] O. Myagmarjav, J. Ryu, Y. Kato, Lithium bromide-mediated reaction performance enhancement of a chemical heat-storage material for magnesium oxide/water chemical heat pumps, Applied Thermal Engineering, 63 (2014) 170-176.
[27] O. Myagmarjav, J. Ryu, Y. Kato, Dehydration kinetic study of a chemical heat storage material with lithium bromide for a magnesium oxide/water chemical heat pump, Progress in Nuclear Energy, 82 (2015) 153-158.
[28] D. Müller, C. Knoll, T. Ruh, W. Artner, J.M. Welch, H. Peterlik, E. Eitenberger, G. Friedbacher, M. Harasek, P. Blaha, K. Hradil, A. Werner, P. Weinberger, Calcium Dotation Facilitates Water Dissociation in Magnesium Oxide, Adv Sus Systems, submitted (2017).
[29] S. Brunauer, P.H. Emmett, E. Teller, Adsorption of Gases in Multimolecular Layers, Journal of the American Chemical Society, 60 (1938) 309-319.
[30] H. Pimminger, G. Habler, N. Freiberger, R. Abart, Evolution of nanostructure and specific surface area during thermally driven dehydration of Mg(OH)2, Physics and Chemistry of Minerals, 43 (2016) 59-68.